Rapid Screening of Cancer Margins in Tissue with Multimodal Confocal Microscopy

Daniel S. Gareau, Ph.D.[1,2], **Hana Jeon, M.D.**[1], **Kishwer S. Nehal, M.D.**[1], and **Milind Rajadhyaksha, Ph.D.**[1]

[1]Memorial Sloan-Kettering Cancer Center Dermatology Service, 160 East 53rd Street, New York, NY 10022

[2]The Rockefeller University, 1230 York Ave, New York, NY 10065

Abstract

Background—Complete and accurate excision of cancer is guided by the examination of histopathology. However, preparation of histopathology is labor intensive and slow, leading to insufficient sampling of tissue and incomplete and/or inaccurate excision of margins. We demonstrate the potential utility of multimodal confocal mosaicing microscopy for rapid screening of cancer margins, directly in fresh surgical excisions, without the need for conventional embedding, sectioning or processing.

Materials/Methods—A multimodal confocal mosaicing microscope was developed to image basal cell carcinoma margins in surgical skin excisions, with resolution that shows nuclear detail. Multimodal contrast is with fluorescence for imaging nuclei and reflectance for cellular cytoplasm and dermal collagen. Thirtyfive excisions of basal cell carcinomas from Mohs surgery were imaged, and the mosaics analyzed by comparison to the corresponding frozen pathology.

Results—Confocal mosaics are produced in about 9 minutes, displaying tissue in fields-of-view of 12 mm with 2X magnification. A digital staining algorithm transforms black and white contrast to purple and pink, which simulates the appearance of standard histopathology. Mosaicing enables rapid digital screening, which mimics the examination of histopathology.

Conclusions—Multimodal confocal mosaicing microscopy offers a technology platform to potentially enable real-time pathology at the bedside. The imaging may serve as an adjunct to conventional histopathology, to expedite screening of margins and guide surgery toward more complete and accurate excision of cancer.

Introduction

Precise and complete excision of cancer is guided by the examination of margins with histopathology during surgery. The preparation of histopathology, however, is labor-intensive and time-consuming. For example, Mohs surgery is a tissue-sparing procedure for nonmelanoma skin cancers[1–3] that is guided by the examination of frozen sections of excision margins. Multiple serial excisions are often necessary to achieve cancer free

Daniel Gareau, Ph. D. dgareau@rockefeller.edu, 1230 York Ave, Mailbox 178, New York NY, 10065, Work: 212 327 7983, Cell/Home: 503 708 7078, Fax: 212 327 8232.

margins, with frozen tissue preparation requiring 20–45 minutes for each excision[4]. In the general surgery setting, however, the preparation of frozen sections is often not possible, and the final margin status is determined with fixed tissue sections, which typically requires several days to prepare. Consequently, sampling of tissue during surgery is often insufficient and cancer margins remain incompletely excised in patients, who must subsequently return for re-excision and/or chemotherapy and/or radiotherapy. Recent studies report that 20–70% of patients undergoing breast cancer lumpectomy may be recalled for re-excision[5]. Following head and neck surgery, 15–50% of patients may present with positive margins and undergo subsequent radio- and/or chemotherapy[6]. The rate of re-excision for positive margins for nonmelanoma skin cancers can be 32–39% following surgical excision[7]. For cutaneous squamous cell carcinomas, the re-excision rate can be 17% following the initial surgery and 28% following the second surgery[8].

The preparation of histopathology requires a laboratory with specialized personnel and expertise and associated expense. For example, for one million Mohs surgeries performed every year in the USA alone, the total treatment cost exceeds $1 billion[9,7]. About 10–20% of the total cost is related to preparation of frozen histopathology, which amounts to about $100–200 million per year. In other surgical settings, the need for subsequent re-excision and/or therapy increases the cost with additional procedures and pathology. In today's environment, the medical profession is facing increasing demands to provide increasingly efficient care at increasingly lower costs. Toward addressing these issues, emerging innovations in noninvasive optical imaging technologies may prove useful. One such emerging technology is confocal mosaicing microscopy that images nuclear and cellular detail, similar to that seen in histopathology, but directly in fresh tissue, without the need for any processing. Confocal mosaicing microscopy was originally developed for detecting basal cell carcinomas (BCCs) in Mohs surgical skin excisions[4, 10–12] and more recently for detection of ductal carcinomas *in situ* and invasive lobular carcinomas in breast biopsies.[13,14]

A confocal microscope noninvasively images a thin plane directly in fresh tissue without the need for traditional grossing, embedding, physical sectioning and staining.[15] Noninvasive imaging of thin planes within whole tissue is called "optical sectioning," and may be performed directly on patients *in vivo* or in freshly excised tissue *ex vivo*. Nuclear and cellular detail is observed in 1–3 μm thin optical sections, with 0.5–1.0 μm resolution. The optical sectioning and resolution is comparable to the typical 5 μm-thin tissue sections that are prepared for histopathology. However, in microscopy, the physics of light fundamentally restrict the ability to perform optical sectioning at high resolution to relatively small fields-of-view of up to 1 mm. To increase the field-of-view, a two-dimensional sequence of images may be acquired and stitched, in software, into a mosaic.[4, 10–12] Mosaics display large areas of tissue at varying magnifications of 2–30X, analogous to that provided by microscope objectives when viewing pathology.

Clinical imaging of skin excisions is an excellent model for testing confocal microscopy and producing a technology platform for translation to other tissues. Feasibility of screening cancer margins, with fluorescence confocal mosaicing microscopy, has been demonstrated for BCCs in Mohs surgical skin excisions.[4, 10–12] Acridine orange was used to stain nuclei in fluorescence contrast, and BCCs were detected with sensitivity of 96.6% and specificity of 89.2%.[16, 17] Although these results are promising, barriers toward routine clinical use may be anticipated. Confocal mosaics are based on a single mode of contrast (fluorescence) and appear in grayscale (black and white), whereas hematoxylin-and-eosin (H&E)-stained histopathology is based on two agents, with hematoxylin staining nuclei purple and eosin staining cytoplasm pink. The grayscale (black-and-white) appearance of confocal mosaics

may pose limitations for acceptance by surgeons and pathologists, who, of course, are trained and accustomed to the purple and pink appearance of histopathology.

Toward addressing this barrier, we report an advance in confocal mosaicing microscopy: a multimodal imaging system with digital staining, to transform grayscale black-and-white contrast to purple and pink, to mimic the appearance of H&E-stained histopathology. Multimodal refers to two modes of contrast: fluorescence contrast to highlight nuclear morphology and reflectance contrast to highlight cellular cytoplasm and dermal morphology. Feasibility is demonstrated for the detection of BCCs margins in Mohs surgical skin excisions.

Materials and Methods

In the Mohs surgery setting, fresh frozen tissue that remains after the preparation of histopathology is routinely discarded. Discarded tissue specimens were collected from thirty-five cases, under an IRB-approved protocol. The frozen tissue specimens were thawed and rinsed with isotonic saline. Acridine orange solution of concentration 1 milliMolar, in phosphate buffered saline at ph 6.0, was used to stain nuclei. As described in our earlier papers[11], the tissue specimens were immersed in acridine orange for 20 seconds and then rinsed in saline to wash off any unbound excess. This staining procedure does not have any adverse effect on subsequent frozen Mohs histopathology.[11] The specimens are mounted in a tissue fixture in the confocal microscope, in a manner that mimics the conventional process of mounting Mohs surgical excisions in a cryostat when preparing frozen sections. The tissue fixture was specially designed and engineered for mounting of Mohs surgical excisions.[10]

A research breadboard version of a commercially available reflectance confocal microscope (Vivascope 2000, Lucid Inc.) was modified to incorporate imaging in fluorescence and mosaicing capability, and details are available elsewhere.[11] Briefly, the microscope is equipped with a 40 mW, 488-nm Argon-ion laser (Omnichrome) for illumination, and two detection channels for fluorescence and reflectance with avalanche photodiode detectors (Perkin-Elmer, Quebec, Canada). Images were acquired at the rate of 20 frames per second. Imaging was performed using a 30X, 0.9 NA objective lens (Stableview, Lucid Inc.) using a water-based gel (Suave Naturals) as an immersion medium. With this lens, the estimated optical sectioning is ~1 μm and the lateral resolution is ~0.3 μm. With the tissue fixture on a translation stage and using a step-and-capture algorithm, up to 36×36 images were acquired, processed and stitched into a mosaic with an algorithm developed in Matlab (Mathworks Inc.).[11] Mosaics display a large field of view in which nuclear detail is visualized. This field-of-view corresponds to a magnification of 2X, as on a standard microscope. Currently, confocal mosaics that display up to 12×12 mm of tissue can be produced in about 9 minutes. Co-registered mosaics were acquired using both the reflectance and fluorescence channels of the multimodal confocal microscope, as described previously.[11] Digital staining was implemented on the reflectance and fluorescence mosaics to simulate H&E-like appearance.

Digital staining transforms the grayscale fluorescence and reflectance pixel intensities into corresponding red, green and blue levels[18], according to the equation: $I_{x,y,k}=1-F_{x,y}(1-H_k)-R_{x,y}(1-E_k)$. The digitally stained image ($I_{x,y,k}$) is a linear combination of the fluorescence ($F_{x,y}$) and reflectance ($R_{x,y}$) mosaics. In this equation, $F_{x,y}$ are the pixel grayscale values for nuclei in the fluorescence mosaic and $R_{x,y}$ are for cellular cytoplasm and collagen in the reflectance mosaic. F and R were single values for each pixel, normalized to make the brightest pixel unity. The subscripts x and y denote the pixel location in the mosaic and the subscript k denotes the bit-depth for red (k=1), green (k=2) and blue (k=3) channels of the digitally stained image. The relative red, green and blue

components to mimic H&E-like appearance were determined from a digital image of a conventional H&E-stained Mohs frozen section by sampling one typical pixel in the hematoxylin-stained area and one in the eosin-stained area. The red, green and blue [R, G, B] components obtained to approximate H&E colors were: H = [0.30, 0.20, 1] and E = [1, 0.55, 0.88].

Application of the equation to each pixel of the grayscale images yields the digitally stained image, in which nuclei appear purple, and collagen and cytoplasm appear pink. The reflectance and fluorescence brightness in confocal images is inverted to the absorbance-based contrast that is seen in histopathology, which is familiar to surgeons and pathologists. In the absence of a fluorescent or reflectance signal, R = F = 0 such that the digitally stained image $I_{x,y,k}$ is unity, which mimics the white background in conventional H&E histopathology. When R and F are not zero, their magnitude determines the suppression of brightness (i. e. absorbance) in $I_{x,y,k}$. If the density of contrast agent (i.e., fluorescent acridine orange molecules that are bound to the nuclei or reflective structures such as cytoplasmic organelles or collagen) is high, the F or R values in the fluorescent and reflectance confocal mosaics are high (i. e., bright on a dark background) and the corresponding digitally stained image appears dark or colored on a bright background.

The digitally stained mosaics were displayed, for examination by the Mohs surgeon, on a 30-in. flat-screen monitor (Dell 222-7175 with a GeForce 8800 GTS video card) consisting of 2500X1600 pixels. The pixilation of this monitor mimics that in a 2X-magnified view of histopathology in a standard microscope. Zoom and pan capabilities, similar to those in today's digital cameras, allow areas of interest to be viewed with variable magnification of 2X to 30X, while maintaining resolution for visualizing nuclear detail. The digital display and observation of mosaics thus mimics the Mohs surgeon's routine for examination of histopathology.

Of the thirty five cases, fourteen were discarded due to poor quality (inconsistent registration, stitching and appearance) of the reflectance mosaics. The remaining twenty one contained BCC margins with varying tumor burden, from grossly positive (i.e. >90%) to largely tumor-free (i.e. <10%). These mosaics were presented to the Mohs surgeon for evaluation of image quality (consistent contrast & seamless mosaic stitching) and screening while remaining "blinded" to the histopathology. The evaluation for presence or absence of BCC margins were subsequently compared to the corresponding frozen pathology.

Results

Figure 1 shows an example of a digitally stained confocal mosaic (figure 1a) and the corresponding H&E-stained Mohs frozen histopathology (figure 1b) at 2× magnification. In the mosaic, nuclei appear purple while cellular cytoplasm and collagen appear pink, comparable to the appearance in standard H&E-stained Mohs histopathology. Normal skin structures such as the epidermis and dermis containing hair follicles, sebaceous glands and collagen are easily recognized. Aggregates of BCC tumors displaying nodular, micronodular and infiltrative subtypes with associated inflammatory infiltrate are readily distinguished from the normal structures. Nuclear and morphologic detail may not be easily appreciated in the small figure in this paper but is readily seen on our large monitor. The details will be more evident in the smaller portions of the mosaic (i. e., insets in figure 1) that are shown in figures 2 and 3.

Figure 2 highlights the production process of a digitally stained confocal mosaic. The exogenous fluorescence mode (figure 2a) with acridine orange displays bright nuclei, which are digitally stained purple. The endogenous reflectance mode (figure 2b) shows

predominantly cellular cytoplasm and collagen in the dermis, which is digitally stained pink. Figure 2c shows the resulting mosaic, which compares well, overall, to the corresponding Mohs histopathology (figure 2d) for the presence and appearance of BCC tumor, normal epidermis and associated features.

Figure 2 also demonstrates digital "zooming" into the mosaic, which allows observation of tissue in submosaics at a higher magnification of 10X, while maintaining full resolution and pixelation. The malignant nuclear morphology of BCC (figure 2c) such as nuclear pleomorphism, increased nuclear density and peripheral palisading is visualized with definition similar to that (figure 2d) seen in the Mohs H&E-stained histopathology. Figure 3 shows these details at higher magnification of 20X, along with the corresponding histopathology.

The appearance of the hematoxylin-stained purple-appearing nuclei is reasonably consistent but the eosin-stained pink-appearing dermis is more variable. This variability appears to be due to the presence of small amounts of acridine orange that may not be completely washed out, resulting in an exogenous fluorescence signal that contaminates the endogenous reflectance image. Thus, there is a purplish component in the dermis that obscures the pink, in some mosaics (figure 1). Elastin fibrils are occasionally stained by acridine orange, leading to a purple fibrous component in the dermis, particularly with solar elastosis in aged and sun-damaged skin. In such cases, the delineation between elastosis and healthy collagen was uncertain. Other artifacts include saturated fluorescence contrast resulting from excess pooling of the acridine orange and/or high laser power.

The consistency of the contrast in the reflectance mode suffered only when the imaging plane was too superficial, picking up artifact reflectance from the glass window onto which the Mohs excision was placed. The consistency of contrast in the fluorescence mode suffered with uneven staining such that, in some areas, the nuclear morphology was too bright (saturated), and, in other areas, too dim (faded). In the review by the Mohs surgeon (co-author KN), who compared the confocal mosaics against the expectations of histology, 9 of the 21 were deemed to be of "poor" quality, 8 were of "medium" quality and 4 were of "good" quality.

The screening results for the 21 mosaics (that all contained BCC tumor margins) were: 17 positive, 4 negative. The 4 mosaics, in which BCCs were present but not identified by the Mohs surgeon, were all cases of very low tumor burden. The fractions of the images that contained tumor within the mosaics were (3/150, 1/350, 4/450 and 2/150), indicating tumor burden of 0.3–2%. Two of these 4 cases were superficial, in which the BCC was budding off the epidermis, and two were micronodular with just one small tumor focus in the dermis. In 3 of the 4 cases that were misread as negative, the quality of the staining was poor: the acridine orange fluorescence (depth of the purple color) showing nuclear detail was weak compared to the strong reflectance (pink) color that showed cellular and dermal collagen detail. Thus, the conclusion from this preliminary clinical review is that the technology - methods for preparation of mosaics and for digital staining - must be further improved to subsequently allow a rigorous study of sensitivity and specificity.

DISCUSSION

Previously, in purely reflectance contrast[10,12] with the use of acetic acid (acetowhitening) to brighten nuclear morphology, large nodular BCC tumors could be detected but since the tumors weren't many fold brighter than the background dermis, small tumors such as micronodular, infiltrating and sclerosing BCCs remained hidden in the mosaic's large field of view. Subsequently, in purely fluorescence contrast with the use of acridine orange, all

subtypes of BCC tumors were detected.[11] Sensitivity and specificity were shown to be 96.6% and 89.2%, respectively.[16,17] Despite the high sensitivity and specificity, black and white (grayscale) images pose a possible barrier to clinical acceptance in that they lack the familiar appearance that surgeons and pathologists are accustomed to, hence re-training is necessary. To address this limitation, we developed a digital staining approach.[18]

This study represents the first step toward a preclinical analysis of multimodal mosaics that appear in purple and pink contrast, similar to that of conventional H&E-stained histopathology, instead of the usual black and white (grayscale) that is commonly seen in confocal microscopy. In our results, unevenness of staining represents a major limitation. The staining protocol needs to be improved to enable consistently strong nuclear contrast. In addition, work is also necessary to improve both the mosaicing approach and the multimodal digital staining approach.

Our ongoing research and engineering is therefore focused on five areas: (i) improvements in image alignment, registration and stitching to produce consistently high quality and clinically acceptable mosaics, (ii) optimization of the fluorescence staining technique with acridine orange, to reduce the purple-staining artifacts in the dermis; (iii) spectral classification analysis of hematoxylin-stained and eosin-stained tissue, to lead to a better understanding of the staining process in histopathology and subsequent improvement in our digital staining algorithm[19]; (iv) refinements in the tissue fixture to enable use for a diverse variety of excision sizes and shapes, in diverse surgical and clinical settings; and (v) development of a "strip mosaicing" approach that will allow display of larger areas of tissue in shorter times, by stitching together long strips of images, similar to the operation in a document scanner[20]. Preliminary results suggest that up to 25×25 mm (1×1 inch) of tissue may be mosaiced in 2–3 minutes.

The limitations of "static" mosaicing in this study may be alleviated with "live" confocal microscopy, where the surgeon would be able to interrogate the tissue in real-time during surgery. While observing a "live" mosaic, regions of uncertainty or artifact could be further investigated by imaging deeper into the tissue, in a manner that mimics the examination of additional sections in histopathology. For example, the uncertain differentiation between hair follicles versus micronodular BCCs in Mohs surgery is traditionally addressed by viewing successive frozen sections in depth. Correspondingly, in a "live" mosaic, the optical section may be focused deeper for real-time observation to depths of 50–100 μm – which would be the equivalent of examining 10–20 histopathology sections.

The present research in skin tissue from Mohs surgery demonstrates proof-of-concept and the possible utility of high-speed large-area mosaicing in many other surgical and clinical settings to examine freshly excised tissue. The technology may enable rapid pathology at the bedside, to potentially expedite and guide surgery or biopsy. Additionally, the images and mosaics are in a digital format that is ideal for telepathology, which continues to be developed and increasingly implemented worldwide.[21–22] Confocal mosaicing microscopy may evolve into a powerful adjunct or, perhaps, an entirely new alternative to histopathology.

Beyond mosaicing in excised tissue, confocal imaging may be performed directly on the patient, pre-operatively and intra-operatively. Our preliminary study indicates the feasibility of detecting residual nonmelanoma skin cancers in patient wounds following shave biopsies.[23] We recently initiated a followup study, to test the feasibility of confocal mapping of nonmelanoma skin cancer margins in patients during Mohs surgery. Ultimately, the best approach may involve clever combinations of "live" mosaicing at the bedside and intra-operative mapping on the patient, configured as needed for any given setting. With

further refinements of this technology to facilitate ease of use, surgeons and clinicians may be empowered to perform more complete screening of margins in a fast, efficient and cost-effective manner.

Acknowledgments

References

1. Minton TJ. Contemporary Mohs surgery applications. Curr Opin Otolaryngo. 2008; 16:376–380.

2. Cumberland L, Dana A, Liegeois N. Mohs micrographic surgery for the management of nonmelanoma skin cancers. Facial Plas Surg Clin N America. 2009; 17:325–335.

3. Perkins W. Who should have Mohs micrographic surgery? Curr Opin Otolaryngo. 2010; 18:283–289.

4. Rajadhyaksha M, Menaker G, Flotte TJ, et al. Rapid confocal examination of nonmelanoma cancers in skin excisions to potentially guide Mohs micrographic surgery. J Invest Dermatol. 2001; 117:1137–1143. [PubMed: 11710924]

5. Jacobs L. Positive margins: the challenge continues for breast surgeons. Ann Surg Oncol. 2008; 15(5):1271–1272. [PubMed: 18320287]

6. Haque R, Contreras R, McNicoll MP, et al. Surgical margins and survival after head and neck cancer surgery. BMC Ear, Nose and Throat Disorders. 2006; 6:2. Available: http://www.biomedcentral.com/1472-6815/6/2. 10.1186/1472-6815-6-2

7. Tierney EP, Hanke CW. Cost effectiveness of Mohs micrographic surgery: review of the literature. J Drugs Dermatol. 2009; 8:914–922. [PubMed: 19852120]

8. Bovill ES, Cullen KW, Barrett W, et al. Clinical and histological findings in re-excision of incompletely excised cutaneous squamous cell carcinoma. J Plast Reconstr Aes. 2009; 62:457–461.

9. Bialy TL, Whalen J, Veledar E, et al. Mohs micrographic surgery versus traditional surgical excision—a cost comparison analysis. Arch Dermatol. 2004; 140:736–742. [PubMed: 15210467]

10. Patel YG, Nehal KS, Aranda I, Li Y, et al. Confocal reflectance mosaicing of basal cell carcinomas in Mohs surgical skin excisions. J Biomed Opt. 2007; 12(3):034027. [PubMed: 17614735]

11. Gareau DS, Li Y, Huang B, Eastman Z, et al. Confocal mosaicing microscopy in Mohs skin excisions: feasibility of rapid surgical pathology. J Biomed Opt. 2008; 13:054001. [PubMed: 19021381]

12. Gareau DS, Patel YG, Li Y, et al. Confocal mosaicing microscopy in skin excisions: a demonstration of rapid surgical pathology. J Microsc. 2009; 233(1):149–159. [PubMed: 19196421]

13. Schiffhauer LM, Boger JN, Bonfiglio TA, et al. Confocal microscopy of unfixed breast needle core biopsies: a comparison to fixed and stained sections. BMC Cancer. 2009; 9:265. [PubMed: 19650910]

14. Maddalena TT, Cabrera MC, Parrish AR, et al. Real-time imaging and characterization of human breast tissue by reflectance confocal microscopy. J Biomed Opt. 2007; 12(5):051901. [PubMed: 17994884]

15. Gonzalez, S.; Gill, M.; Halpern, AC., editors. Reflectance Confocal Microscopy of Cutaneous Tumors. London: Informa U.K. Ltd; 2008.

16. Gareau DS, Karen JK, Dusza SW, et al. Sensitivity and specificity for detecting basal cell carcinomas in Mohs excisions with confocal fluorescence mosaicing microscopy. J Biomed Opt. 2009; 14(3):034012. [PubMed: 19566305]

17. Karen JK, Gareau DS, Dusza SW, et al. Detection of basal cell carcinomas in Mohs excisions with fluorescence confocal mosaicing microscopy. Brit J Dermatol. 2009; 160(6):1242–1250. [PubMed: 19416248]

18. Gareau DS. The feasibility of digitally stained multimodal confocal mosaics to simulate histopathology. J Biomed Opt. 2009; 14(3):034050. [PubMed: 19566342]

19. Bini J, Spain J, Nehal K, Hazelwood V, DiMarzio C, Rajadhyaksha M. Confocal mosaicing microscopy of human skin *ex vivo*: spectral analysis for digital staining to simulate histology-like appearance. J Biomed Opt. 2011; 16:076008. http://dx.doi.org/10.1117/1.3596742. [PubMed: 21806269]

20. Abeytunge S, Li Y, Larson B, Toledo-Crow R, Rajadhyaksha M. Rapid confocal imaging of large areas of excised tissue with strip mosaicing. J Biomed Opt. 2012:050504-1. [PubMed: 22612119]

21. Weinstein RS, Graham AR, Richter LC, et al. Overview of telepathology, virtual microscopy, and whole slide imaging: prospects for the future. Hum Pathol. 2009 Aug; 40(8):1057–1069. [PubMed: 19552937]

22. Jara-Lazaro AR, Thamboo TP, Teh M, et al. Digital pathology: exploring its applications in diagnostic surgical pathology practice. Pathology. 2010; 42(6):512–518. [PubMed: 20854068]

23. Scope A, Mahmood U, Gareau DS, et al. *In vivo* reflectance confocal microscopy of shave biopsy wounds: feasibility of intraoperative mapping of cancer margins. Brit J Dermatol. 2010; 163:1218–28. [PubMed: 20874785]
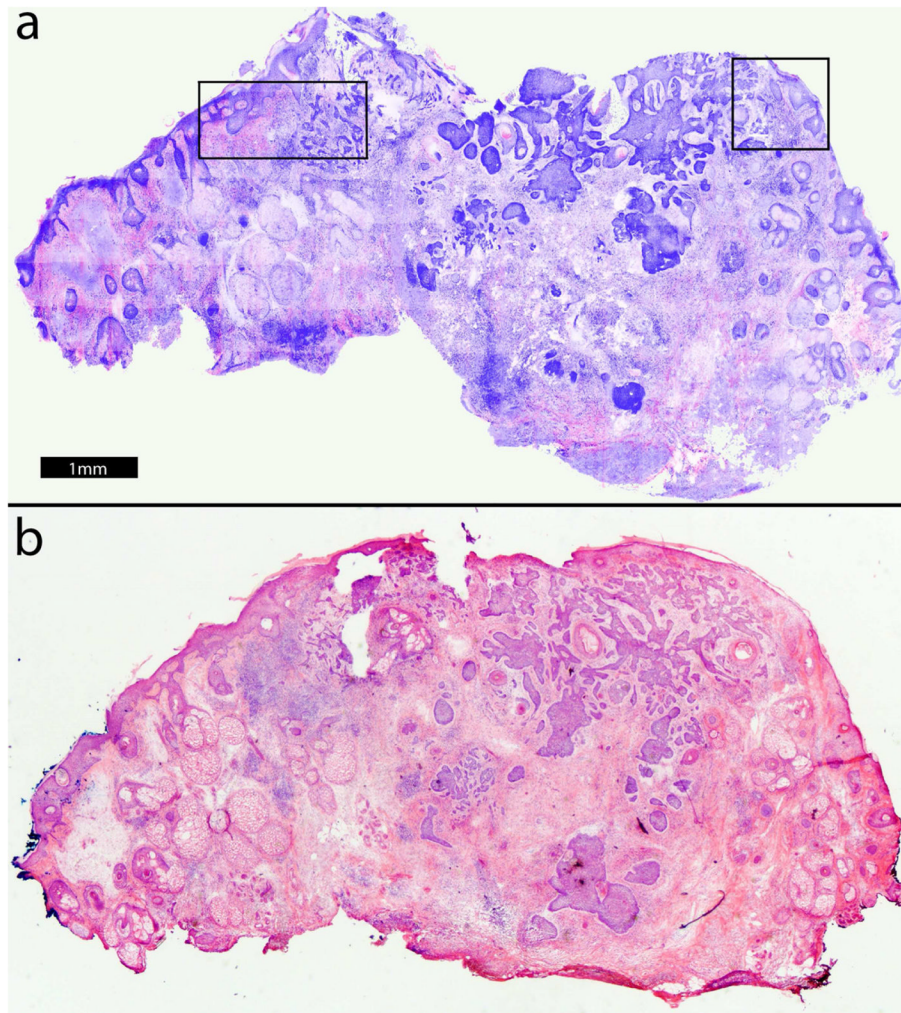
Figure 1.
Digitally stained confocal mosaic with residual BCC (a) compares well to Mohs H&E-stained frozen section histopathology (b, magnification 2×). To make the details more evident, two inset areas are shown at higher magnifications: the upper left at 10X (figure 2) and the upper right at 20X (figure 3).
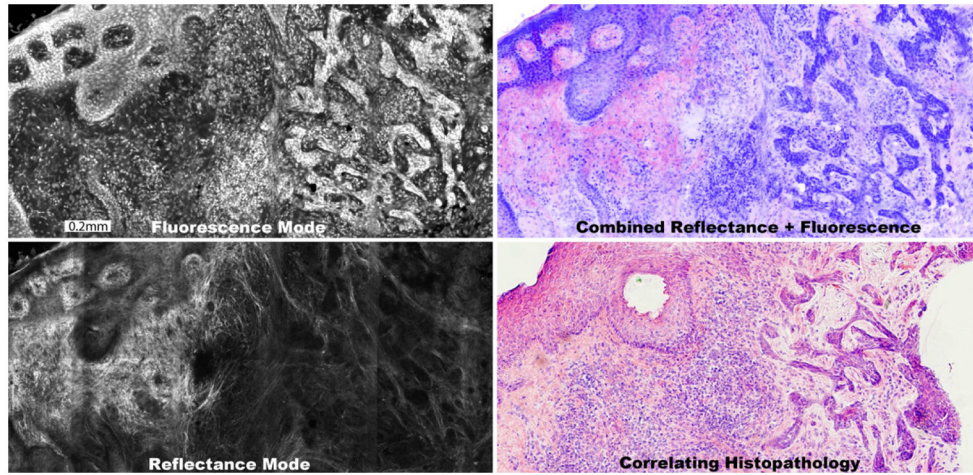
Figure 2.
A digitally stained confocal mosaic is composed of an exogenous fluorescent mosaic showing nuclei stained with acridine orange (a) that is combined with an endogenous reflectance mosaic showing cellular cytoplasm and collagen (b). The fluorescence mosaic is digitally stained purple and the reflectance pink and the two are overlaid to produce the digitally stained mosaic (c). The mosaic appears comparable to the H&E-stained histopathology (d, magnification 10×), for the presence and appearance of BCC tumor, normal epidermis and associated features. The features are further described in figure 3.
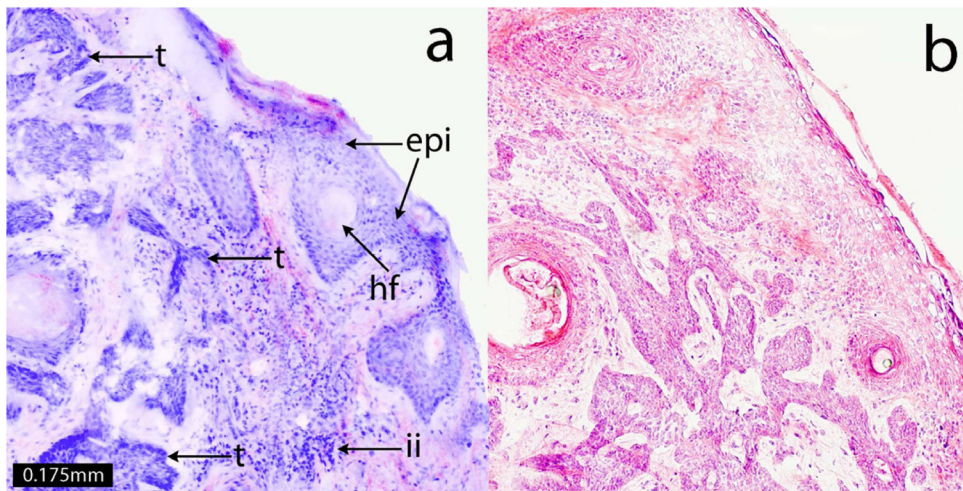
Figure 3.
A digitally stained confocal submosaic shows details of features at 20× magnification (a) that include the epidermis along the edges of the tissue (epi), hair follicle (hf), inflammatory infiltration (ii) and micronodular BCC tumor (t). These features appear similar to those seen in the corresponding H&E-stained histopathology (b, magnification 20×). Such features are routinely examined in Mohs pathology.